

Twin polaritons in semiconductor microcavities

J. Ph. Karr, A. Baas, and E. Giacobino

Laboratoire Kastler Brossel, Université Paris 6, Ecole Normale Supérieure et CNRS, UPMC Case 74, 4 Place Jussieu, 75252 Paris Cedex 05, France

(Received 9 February 2004; published 9 June 2004)

The quantum correlations between the beams generated by polariton pair scattering in a semiconductor microcavity above the parametric oscillation threshold are computed analytically. The influence of various parameters, including the cavity-exciton detuning, the intensity mismatch between the signal and idler beams, and the amount of spurious noise, is analyzed. We show that very strong quantum correlations between the signal and idler polaritons can be achieved. However, the quantum effects in the outgoing light fields are strongly reduced due to the large mismatch in the coupling of the signal and idler polaritons to the external photons.

DOI: 10.1103/PhysRevA.69.063807

PACS number(s): 42.50.Dv, 71.36.+c

I. INTRODUCTION

High finesse semiconductor microcavities with embedded quantum wells allow us to achieve the strong-coupling regime between the quantum-well excitons and the cavity photons [1]. The normal modes are mixed exciton-photon modes, called cavity polaritons, which present large nonlinearities coming from the Coulomb interactions between the exciton components. Under resonant pumping, this leads to a parametric process where a pair of pump polaritons scatter into nondegenerate signal and idler modes while conserving energy and momentum. The scattering is particularly strong in microcavities, because the unusual shape of the polariton dispersion makes it possible for the pump, signal, and idler modes to be on resonance at the same time (see Fig. 1). Moreover, the relationship between the in-plane momentum of each polariton mode and the direction of the external photon to which it couples [2] enables us to investigate the parametric scattering using measurements at different angles to access the various modes.

Parametric processes were demonstrated in semiconductor microcavities by Savvidis *et al.* [3] using ultrafast pump-probe measurements. They observed parametric amplification, where the scattering is stimulated by excitation of the signal mode with a weak probe field. Parametric oscillation, where there is no probe and a coherent population in the signal and idler modes appears spontaneously, has since been observed by Stevenson *et al.* [4] and Baumberg *et al.* [5] in cw experiments. The lower polariton was pumped resonantly at the “magic” angle of about 16° . Above a threshold pump intensity, strong signal and idler beams were observed at about 0° and 35° , without any probe stimulation. The coherence of these beams was demonstrated by a significant spectral narrowing.

The large optical nonlinearity of cavity polaritons makes them very attractive for quantum optics. Noise reduction on the reflected light field has been predicted [6] and achieved experimentally [7] for a resonant pumping of the lower polariton at 0° . The parametric fluorescence was recently predicted to produce strongly correlated pairs of signal and idler polaritons, yielding a two-mode squeezed state [8,9]. The parametric oscillation regime is also very interesting in this

respect [10]. It is well known that optical parametric oscillators (OPOs) can be used to generate twin beams, the fluctuations of which are correlated at the quantum level. A noise reduction of 86% was obtained by subtracting the intensities of the signal and idler beams produced by a LiNbO_3 OPO [11].

The purpose of this paper is to investigate the possibility of generating twin beams using a semiconductor microcavity above the parametric oscillation threshold. The classical model developed by Whittaker [12] is no longer sufficient to study the quantum noise properties of the system. Thus we adapt the quantum model by Ciuti *et al.*, previously used in the context of parametric amplification [13] and parametric fluorescence [9,14], to the parametric oscillator configuration. Furthermore, we compute the field fluctuations using the input-output method [15,16]. We also include the excess noise associated with the excitonic relaxation, not considered by previous authors [9,14], which may play a critical role for experimental observation of the quantum effect.

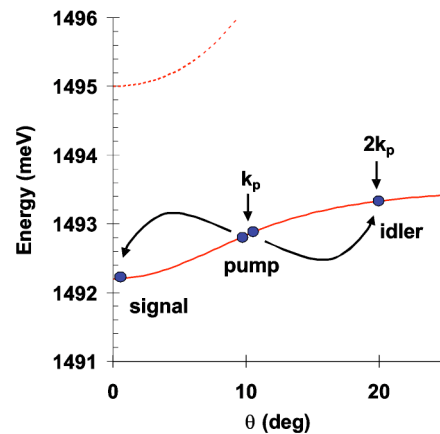


FIG. 1. Energy dispersion of the two polariton branches for a microcavity sample having a Rabi splitting of 2.8 meV at zero cavity-exciton detuning. The arrows show the parametric conversion of the pump polaritons ($\approx 10^\circ$) into signal (0°) and idler ($\approx 20^\circ$) polaritons.

II. MODEL

A. Hamiltonian

Following Ciuti *et al.* [13,14] we write the effective Hamiltonian for the coupled exciton-photon system. The spin degree of freedom is neglected,

$$H = H_0 + H_{exc-exc} + H_{sat}. \quad (1)$$

The first term is the linear Hamiltonian for excitons and cavity photons,

$$H_0 = \sum_{\mathbf{k}} E_{exc}(k) b_{\mathbf{k}}^\dagger b_{\mathbf{k}} + \sum_{\mathbf{k}} E_{cav}(k) a_{\mathbf{k}}^\dagger a_{\mathbf{k}} + \sum_{\mathbf{k}} \hbar \Omega_R (a_{\mathbf{k}}^\dagger b_{\mathbf{k}} + b_{\mathbf{k}}^\dagger a_{\mathbf{k}}), \quad (2)$$

with $b_{\mathbf{k}}^\dagger$ and $a_{\mathbf{k}}^\dagger$ the creation operators, respectively, for excitons and photons of in-plane wave vector \mathbf{k} , which satisfy boson commutation rules. $E_{exc}(k)$ and $E_{cav}(k)$ are the energy dispersions for the exciton and cavity modes. The last term represents the linear coupling between the exciton and cavity photon, which causes the vacuum Rabi splitting $2\hbar\Omega_R$. The fermionic nature of electrons and holes causes a deviation of the excitons from bosonic behavior, which is accounted for through an effective exciton-exciton interaction and exciton saturation. The exciton-exciton interaction term writes

$$H_{exc-exc} = \frac{1}{2} \sum_{\mathbf{k}, \mathbf{k}', \mathbf{q}} V_q b_{\mathbf{k}+\mathbf{q}}^\dagger b_{\mathbf{k}'-\mathbf{q}}^\dagger b_{\mathbf{k}} b_{\mathbf{k}'}, \quad (3)$$

where $V_q \approx V_0 = (6e^2 a_{exc} / \epsilon_0 A)$ for $q a_{exc} \ll 1$, a_{exc} being the two-dimensional exciton Bohr radius, ϵ_0 the dielectric constant of the quantum well, and A the macroscopic quantization area. The saturation term in the light-exciton coupling is

$$H_{sat} = - \sum_{\mathbf{k}, \mathbf{k}', \mathbf{q}} V_{sat} (a_{\mathbf{k}+\mathbf{q}}^\dagger b_{\mathbf{k}'-\mathbf{q}}^\dagger b_{\mathbf{k}} b_{\mathbf{k}'} + a_{\mathbf{k}+\mathbf{q}} b_{\mathbf{k}'-\mathbf{q}} b_{\mathbf{k}}^\dagger b_{\mathbf{k}'}^\dagger), \quad (4)$$

where $V_{sat} = (\hbar \Omega_R / n_{sat} A)$ with $n_{sat} = 7 / (16 \pi a_{exc}^2)$ being the exciton saturation density. We consider resonant or quasi-resonant excitation of the lower polariton branch by a quasimonochromatic laser field of frequency $\omega_L = E_L / \hbar$ and wave vector \mathbf{k}_L . If the pump intensity is not too high the resonances (i.e., the polariton states) are not modified, except for an energy shift (that will be calculated below). Then it is much more convenient to work directly in the polariton basis. The polariton operators are obtained by a unitary transformation of the exciton and photon operators

$$\begin{pmatrix} p_{\mathbf{k}} \\ q_{\mathbf{k}} \end{pmatrix} = \begin{pmatrix} -C_k & X_k \\ X_k & C_k \end{pmatrix} \begin{pmatrix} a_{\mathbf{k}} \\ b_{\mathbf{k}} \end{pmatrix}, \quad (5)$$

where X_k and C_k are positive real numbers called the Hopfield coefficients, given by

$$X_k^2 = \frac{\delta_k + \sqrt{\delta_k^2 + \Omega_R^2}}{2\sqrt{\delta_k^2 + \Omega_R^2}}, \quad (6)$$

$$C_k^2 = \frac{\Omega_R^2}{2\sqrt{\delta_k^2 + \Omega_R^2}(\delta_k + \sqrt{\delta_k^2 + \Omega_R^2})}. \quad (7)$$

X_k^2 and C_k^2 can be interpreted, respectively, as the exciton and photon fraction of the lower polariton $p_{\mathbf{k}}$. In the case of resonant excitation of the lower polariton, it is possible to consider only the lower polariton and neglect its nonlinear coupling to the upper polariton. In terms of the lower polariton operators, the Hamiltonian (1) then reads as

$$H = H_P + H_{PP}^{eff}. \quad (8)$$

H_P is the free-evolution term for the lower polariton

$$H_P = \sum_{\mathbf{k}} E_P(k) p_{\mathbf{k}}^\dagger p_{\mathbf{k}}, \quad (9)$$

and H_{PP}^{eff} is an effective polariton-polariton interaction,

$$H_{PP}^{eff} = \frac{1}{2} \sum_{\mathbf{k}, \mathbf{k}', \mathbf{q}} V_{\mathbf{k}, \mathbf{k}', \mathbf{q}}^{PP} p_{\mathbf{k}+\mathbf{q}}^\dagger p_{\mathbf{k}'-\mathbf{q}}^\dagger p_{\mathbf{k}} p_{\mathbf{k}'}, \quad (10)$$

where

$$V_{\mathbf{k}, \mathbf{k}', \mathbf{q}}^{PP} = \{V_0 X_{|\mathbf{k}+\mathbf{q}|} X_{k'} + 2V_{sat}(C_{|\mathbf{k}+\mathbf{q}|} X_{k'} + C_{k'} X_{|\mathbf{k}+\mathbf{q}|})\} X_{|\mathbf{k}'-\mathbf{q}|} X_k. \quad (11)$$

In the following, we neglect the contribution of the saturation term, which can be shown to be more than an order of magnitude smaller than the polariton-polariton interaction [17]. This yields $V_{\mathbf{k}, \mathbf{k}', \mathbf{q}}^{PP} \approx V_0 X_{|\mathbf{k}+\mathbf{q}|} X_{k'} X_{|\mathbf{k}'-\mathbf{q}|} X_k$. We also neglect multiple diffusions, i.e., interactions between modes other than the pump mode. This approximation is valid not too far above the parametric oscillation threshold.¹ It is equivalent to considering only the terms where the pump polariton operator $p_{\mathbf{k}_L}$ appears at least twice:

$$H_{PP}^{eff} = \frac{1}{2} V_{\mathbf{k}_L, \mathbf{k}_L, 0} p_{\mathbf{k}_L}^\dagger p_{\mathbf{k}_L}^\dagger p_{\mathbf{k}_L} p_{\mathbf{k}_L} + \sum_{\mathbf{k} \neq \mathbf{k}_L} V_{\mathbf{k}_L, \mathbf{k}_L, \mathbf{k}_L - \mathbf{k}} (p_{2\mathbf{k}_L - \mathbf{k}}^\dagger p_{\mathbf{k}}^\dagger p_{\mathbf{k}_L} p_{\mathbf{k}_L} + \text{H.c.}) + 2 \sum_{\mathbf{k} \neq \mathbf{k}_L} V_{\mathbf{k}, \mathbf{k}_L, 0}^{PP} p_{\mathbf{k}_L}^\dagger p_{\mathbf{k}}^\dagger p_{\mathbf{k}_L} p_{\mathbf{k}}. \quad (12)$$

The first term is a Kerr-like term for the polaritons in the pump mode. The second term is a ‘‘fission’’ process, where two polaritons of wave vector \mathbf{k}_L are converted into a ‘‘signal’’ polariton of wave vector \mathbf{k} and an ‘‘idler’’ polariton of wave vector $2\mathbf{k}_L - \mathbf{k}$. The last term corresponds to the interaction of the pump mode \mathbf{k}_L with all the other \mathbf{k} states, which results in a blueshift proportional to $|p_{\mathbf{k}_L}|^2$.

B. Resonance condition

The resonance condition for the fission process $\{\mathbf{k}_L, \mathbf{k}_L\} \rightarrow \{\mathbf{k}, 2\mathbf{k}_L - \mathbf{k}\}$ reads

¹Multiple diffusions were demonstrated in Refs. [24,25].

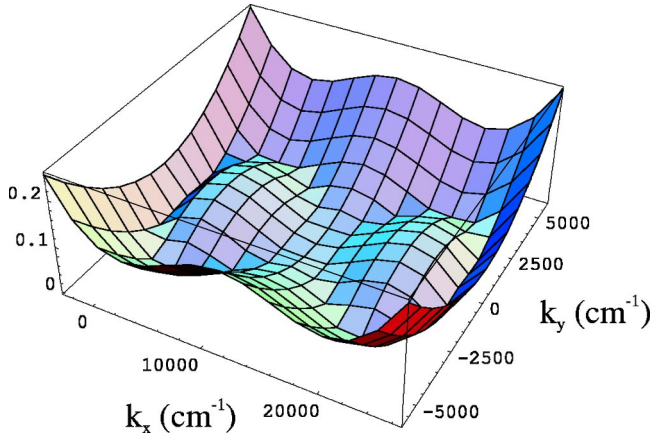


FIG. 2. Plot of the quantity $|E_p(\mathbf{k}) + E_p(2\mathbf{k}_L - \mathbf{k}) - 2E_p(\mathbf{k}_L)|$ (in meV) as a function of k_x and k_y (in cm^{-1}) for the parameters of Fig. 1.

$$\tilde{E}_p(\mathbf{k}) + \tilde{E}_p(2\mathbf{k}_L - \mathbf{k}) = 2\tilde{E}_p(\mathbf{k}_L), \quad (13)$$

where $\tilde{E}_p(\mathbf{q})$ is the energy of the polariton of wave vector \mathbf{q} , renormalized by the interaction with the pump polaritons

$$\tilde{E}_p(\mathbf{q}) = E_p(q) + 2V_{\mathbf{q},\mathbf{k}_L,0} |\langle p_{\mathbf{k}_L} \rangle|^2. \quad (14)$$

Note that the factor of 2 disappears for $\mathbf{q} = \mathbf{k}_L$. Equation (13) always has a trivial solution $\mathbf{k} = \mathbf{k}_L$. Nontrivial solutions exist, provided that the wave vector \mathbf{k}_L is above a critical value, or equivalently, if the angle of incidence is above the so-called “magic angle” θ_c [3]. From now on we suppose that the microcavity is excited resonantly with an angle θ_c . Figure 2 is a plot of the quantity $|E_p(\mathbf{k}) + E_p(2\mathbf{k}_L - \mathbf{k}) - 2E_p(\mathbf{k}_L)|$ as a function of $\mathbf{k} = \{k_x, k_y\}$, with \mathbf{k}_L being parallel to the x axis.

This shows that the resonance condition can be satisfied for a wide range of wave vectors $\{\mathbf{k}, 2\mathbf{k}_L - \mathbf{k}\}$. In recent experiments, parametric oscillation was observed in the normal direction $\mathbf{k} = 0$ [4,19]. In this paper we consider only the parametric process $\{\mathbf{k}_L, \mathbf{k}_L\} \rightarrow \{0, 2\mathbf{k}_L\}$ assuming that the other ones remain below threshold. Then, we can neglect the effect of modes other than $0, \mathbf{k}_L, 2\mathbf{k}_L$. The evolution of these three modes is given by a closed set of equations that we are now going to derive.

III. HEISENBERG-LANGEVIN EQUATIONS

In order to study the quantum fluctuations we have to write the Heisenberg-Langevin equations, including the relaxation and fluctuation terms. The relaxation of the cavity mode comes from the interaction with the external electromagnetic field through the Hamiltonian [18],

$$H_I = i\hbar \int \frac{d\omega}{2\pi} \kappa (a_{\mathbf{k}}^\dagger A_\omega - A_\omega^\dagger a_{\mathbf{k}}). \quad (15)$$

The coupling constant is given by $\kappa = \sqrt{2\gamma_{ak}}$, where γ_{ak} is the cavity linewidth (HWHM). This leads to the following evolution equation for the cavity field in an empty cavity:

$$\frac{da_{\mathbf{k}}(t)}{dt} = -\gamma_{ak} a_{\mathbf{k}}(t) + \sqrt{2\gamma_{ak}} A_{\mathbf{k}}^{in}(t), \quad (16)$$

where $A_{\mathbf{k}}^{in}(t)$ is the incoming coherent laser field, which has fluctuations equal to the vacuum noise. In this equation the normalizations are not the same for the cavity field as for the external field: $n_{a_{\mathbf{k}}}(t) = \langle a_{\mathbf{k}}^\dagger(t) a_{\mathbf{k}}(t) \rangle$ is the mean number of cavity photons, while $I_{\mathbf{k}}^{in} = \langle A_{\mathbf{k}}^{in\dagger}(t) A_{\mathbf{k}}^{in}(t) \rangle$ is the mean number of incident photons per second.

Exciton relaxation is a much more complex problem. The density is assumed to be low enough to neglect the relaxation due to exciton-exciton interaction [20]. At low density and low enough temperature the main relaxation mechanism is the interaction with acoustic phonons. A given exciton mode $b_{\mathbf{k}}$ is coupled to all the other exciton modes $b_{\mathbf{k}'}$, and to all the phonon modes fulfilling the condition of energy and wave-vector conservation [21]. Relaxation in microcavities in the strong-coupling regime has been studied in detail [22,23]. However, the derivation of the corresponding fluctuation terms requires additional hypotheses [10]. We model the relaxation by a linear coupling to the exciton reservoir (made of all the exciton modes $b_{\mathbf{k}'}$, with $\mathbf{k}' \neq \mathbf{k}$), which is assumed to be harmonic.² Then, in the same way as for the photon field, the fluctuation-dissipation part in the Langevin equation for the excitons writes

$$\frac{db_{\mathbf{k}}(t)}{dt} = -\gamma_{bk} b_{\mathbf{k}}(t) + \sqrt{2\gamma_{bk}} B_{\mathbf{k}}^{in}(t), \quad (17)$$

where γ_{bk} is the exciton linewidth (HWHM) and $B_{\mathbf{k}}^{in}(t)$ the input excitonic field, which is a linear combination of the reservoir modes. Since there is no direct excitation of the exciton field, it comprises only noise, which is at least the vacuum noise (in the case where the exciton reservoir is the vacuum state).

Using these results we can write the Heisenberg-Langevin equations for the cavity and exciton modes of wave vectors $0, \mathbf{k}_L, 2\mathbf{k}_L$ and then for the three corresponding lower polariton modes. We define the slowly varying operators,

$$\tilde{p}_{\mathbf{k}_L}(t) = p_{\mathbf{k}_L}(t) e^{iE_L t/\hbar},$$

$$\tilde{p}_0(t) = p_0(t) e^{iE_p(0)t/\hbar},$$

$$\tilde{p}_{2\mathbf{k}_L}(t) = p_{2\mathbf{k}_L}(t) e^{iE_p(2\mathbf{k}_L)t/\hbar}, \quad (18)$$

which obey the following equations:

$$\begin{aligned} \frac{d\tilde{p}_0}{dt} &= -\frac{i}{\hbar} (2V_{0,\mathbf{k}_L,0} \tilde{p}_{\mathbf{k}_L}^\dagger \tilde{p}_{\mathbf{k}_L} - i\gamma_0) \tilde{p}_0 \\ &\quad - \frac{i}{\hbar} V_{\mathbf{k}_L,\mathbf{k}_L,\mathbf{k}_L} \tilde{p}_{2\mathbf{k}_L}^\dagger \tilde{p}_{\mathbf{k}_L}^2 e^{i\Delta E t/\hbar} + P_0^{in}, \end{aligned} \quad (19)$$

²The effect of the phonon reservoir is included only in the coupling coefficient; as a result, this model does not allow us to study the temperature dependence of the fluctuations.

$$\begin{aligned} \frac{d\tilde{p}_{2\mathbf{k}_L}}{dt} = & -\frac{i}{\hbar}(2V_{2\mathbf{k}_L,\mathbf{k}_L,0}\tilde{p}_{\mathbf{k}_L}^\dagger\tilde{p}_{\mathbf{k}_L} - i\gamma_{2k_L})\tilde{p}_{2\mathbf{k}_L} \\ & -\frac{i}{\hbar}V_{\mathbf{k}_L,\mathbf{k}_L,\mathbf{k}_L}\tilde{p}_0^\dagger\tilde{p}_{\mathbf{k}_L}^2 e^{i\Delta E t/\hbar} + P_{2\mathbf{k}_L}^{in}, \end{aligned} \quad (20)$$

$$\begin{aligned} \frac{d\tilde{p}_{\mathbf{k}_L}}{dt} = & -\frac{i}{\hbar}(\Delta_L + V_{\mathbf{k}_L,\mathbf{k}_L,0}\tilde{p}_{\mathbf{k}_L}^\dagger\tilde{p}_{\mathbf{k}_L} - i\gamma_{k_L})\tilde{p}_{\mathbf{k}_L} \\ & -\frac{2i}{\hbar}V_{\mathbf{k}_L,\mathbf{k}_L,\mathbf{k}_L}\tilde{p}_{\mathbf{k}_L}^\dagger\tilde{p}_0\tilde{p}_{2\mathbf{k}_L} e^{-i\Delta E t/\hbar} + P_{\mathbf{k}_L}^{in}, \end{aligned} \quad (21)$$

where for any given wave vector \mathbf{q} , $P_{\mathbf{q}}^{in} = -C_q\sqrt{2\gamma_{aq}}A_{\mathbf{q}}^{in} + X_q\sqrt{2\gamma_{bq}}B_{\mathbf{q}}^{in}$ is the polariton input field (which is a linear combination of the cavity and exciton input fields; only the driving laser field $A_{\mathbf{k}_L}^{in}$ has a nonzero mean value), $\gamma_q = C_q^2\gamma_{aq} + X_q^2\gamma_{bq}$ is the polariton linewidth; $\Delta_L = E_p(k_L) - E_L$ is the laser detuning; and $\Delta E = E_p(2k_L) + E_p(0) - 2E_L$ is the energy mismatch.

Compared to previous treatments [9,14], the model includes a full treatment of the field fluctuations. In addition, it is valid above threshold since the equation of motion of the pumped mode accounts for the pump depletion. As mentioned above, this is valid not too far above threshold, because otherwise multiple scattering cannot be neglected anymore [24,25].

This set of equations is similar to the evolution equations of a nondegenerate triply resonant optical parametric oscillator [26]. The nonlinearity is of $\chi^{(3)}$ type, while in most OPOs it is of $\chi^{(2)}$ type. OPOs based on four-wave mixing have already been demonstrated [27]. However, let us stress that here the parametric process involves the excitations of a semiconductor matter wave (i.e., polaritons) instead of photons. In the following, we evaluate the potential applications of this type of OPO in quantum optics. The hybrid nature of polaritons makes the treatment of quantum fluctuations more complicated, since we have to consider additional sources of noise (i.e., the luminescence of excitons).

IV. MEAN FIELDS ABOVE THRESHOLD

The first task is to compute the stationary state of the system. This comes to the calculation done by Whittaker in Ref. [12]. We neglect the renormalization effects due to the interaction with the pump mode, which allows us to get analytical expressions. We suppose that the angle of incidence is adjusted in order to satisfy the resonance condition $\Delta E = 0$ and that the pump laser is perfectly resonant ($\Delta_L = 0$). Equations (19)–(21) now write

$$\frac{d\tilde{p}_0}{dt} = -\gamma_0\tilde{p}_0 - iE_{int}\tilde{p}_{2\mathbf{k}_L}^\dagger\tilde{p}_{\mathbf{k}_L}^2 + P_0^{in}, \quad (22)$$

$$\frac{d\tilde{p}_{2\mathbf{k}_L}}{dt} = -\gamma_{2k_L}\tilde{p}_{2\mathbf{k}_L} - iE_{int}\tilde{p}_0^\dagger\tilde{p}_{\mathbf{k}_L}^2 + P_{2\mathbf{k}_L}^{in}, \quad (23)$$

$$\frac{d\tilde{p}_{\mathbf{k}_L}}{dt} = -\gamma_{k_L}\tilde{p}_{\mathbf{k}_L} - 2iE_{int}\tilde{p}_{\mathbf{k}_L}^\dagger\tilde{p}_0\tilde{p}_{2\mathbf{k}_L} + P_{\mathbf{k}_L}^{in}, \quad (24)$$

where $E_{int} = V_{\mathbf{k}_L,\mathbf{k}_L,\mathbf{k}_L}/\hbar$. Let us recall that among the polariton input fields, only the photon part of $P_{\mathbf{k}_L}^{in}$ corresponding to the pump laser field has a nonzero mean value. The excitonic input fields $B_{\mathbf{q}}^{in}$ correspond to the thermal excitation of the exciton modes (that eventually gives rise to luminescence) and are incoherent fields with zero mean value. The stationary state is given by

$$-\gamma_{k_L}\tilde{p}_{\mathbf{k}_L} - 2iE_{int}\tilde{p}_{\mathbf{k}_L}^*\tilde{p}_0\tilde{p}_{2\mathbf{k}_L} = C_{k_L}\sqrt{2\gamma_a}\bar{A}_{\mathbf{k}_L}^{in}, \quad (25)$$

$$-\gamma_0\tilde{p}_0 - iE_{int}\tilde{p}_{2\mathbf{k}_L}^*\tilde{p}_{\mathbf{k}_L}^2 = 0, \quad (26)$$

$$-\gamma_{2k_L}\tilde{p}_{2\mathbf{k}_L}^* + iE_{int}\tilde{p}_0\tilde{p}_{\mathbf{k}_L}^{*2} = 0. \quad (27)$$

For a nontrivial solution to exist, the determinant of the last two equations must be zero,

$$E_{int}^2|\tilde{p}_{\mathbf{k}_L}|^4 - \gamma_0\gamma_{2k_L} = 0, \quad (28)$$

which gives the pump-polariton population threshold

$$|\tilde{p}_{\mathbf{k}_L}|^2 = \frac{\sqrt{\gamma_0\gamma_{2k_L}}}{E_{int}}, \quad (29)$$

and the pump intensity threshold

$$I_{\mathbf{k}_L,thr}^{in} = |\bar{A}_{\mathbf{k}_L,thr}^{in}|^2 = \frac{\gamma_{k_L}^2(\gamma_0\gamma_{2k_L})^{1/2}}{2\gamma_a C_{k_L}^2 E_{int}}. \quad (30)$$

The signal and idler polariton populations are easily derived,

$$|\tilde{p}_0|^2 = \frac{\gamma_{k_L}}{2E_{int}}\sqrt{\frac{\gamma_{2k_L}}{\gamma_0}}(\sigma - 1), \quad (31)$$

$$|\tilde{p}_{2\mathbf{k}_L}|^2 = \frac{\gamma_{k_L}}{2E_{int}}\sqrt{\frac{\gamma_0}{\gamma_{2k_L}}}(\sigma - 1), \quad (32)$$

where $\sigma = \sqrt{I_{\mathbf{k}_L}^{in}/I_{\mathbf{k}_L,thr}^{in}}$ is the pump parameter. We finally get the intensities of the signal and idler output light fields,

$$I_0^{out} = 2\gamma_a C_0^2 |\tilde{p}_0|^2 = \frac{\gamma_a \gamma_{k_L} C_0^2}{E_{int}} \sqrt{\frac{\gamma_{2k_L}}{\gamma_0}} (\sigma - 1),$$

$$I_{2\mathbf{k}_L}^{out} = 2\gamma_a C_{2k_L}^2 |\tilde{p}_{2\mathbf{k}_L}|^2 = \frac{\gamma_a \gamma_{k_L} C_{2k_L}^2}{E_{int}} \sqrt{\frac{\gamma_0}{\gamma_{2k_L}}} (\sigma - 1). \quad (33)$$

Above threshold, all the polaritons created by the pump are transferred to the signal and idler modes, so that the number of pump polaritons is clamped to a fixed value. This phenomenon, called pump depletion, is well known in triply resonant OPOs. The signal and idler intensities grow like $\sqrt{I_{\mathbf{k}_L}^{in}}$ (see Fig. 3). These results are in agreement with those of Ref. [12].

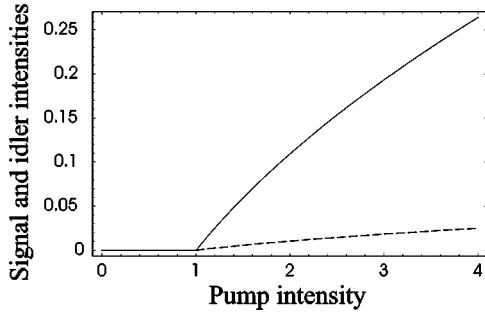


FIG. 3. Intensities of the output signal (solid line) and idler (dashed line) beams as a function of the pump intensity. All the intensities are normalized to the threshold intensity $I_{\mathbf{k}_L}^{in,thr}$. The three modes are assumed to have the same linewidths.

Finally, we study the ratio of the signal and idler output intensities, which is an important parameter in view of the analysis of the correlations between these two beams. It is given by the simple equation,

$$\frac{I_0^{out}}{I_{2\mathbf{k}_L}^{out}} = \frac{\gamma_{2k_L} C_0^2}{\gamma_0 C_{2k_L}^2}. \quad (34)$$

We consider a typical III-V microcavity sample containing one quantum well, with a Rabi splitting $2\hbar\Omega_R = 2.8$ meV. At zero cavity-exciton detuning, one finds $k_L = 1.15 \times 10^4$ cm⁻¹. The photon fractions of the signal and idler modes are, respectively, $C_0^2 = 0.5$ and $C_{2k_L}^2 \approx 0.053$. Assuming that they have equal linewidths the signal beam power should be about 10 times that of the idler beam. It is possible to reduce this ratio by increasing the cavity-exciton detuning, as can be seen in Fig. 4. However, the oscillation threshold goes up. In the following, all the results will be given at zero detuning.

V. FLUCTUATIONS

A. Linearized evolution equations

For any operator $O(t)$ we define a fluctuation operator $\delta O(t) = O(t) - \langle O(t) \rangle$. In order to compute the fluctuations, we use the “semiclassical” linear input-output method, which consists of studying the transformation of the incident fluctuations by the system [16]. It has been shown to be equivalent

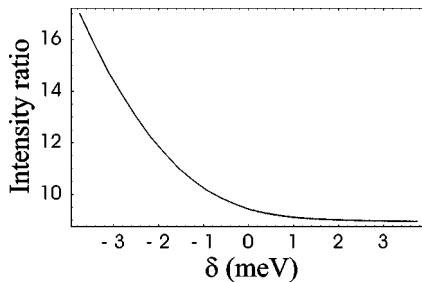


FIG. 4. The ratio of the photonic fractions of the signal and idler polaritons as a function of the cavity-exciton detuning δ . The Rabi splitting is 2.8 meV.

to a full quantum treatment. We linearize Eqs. (22)–(24) in the vicinity of the working point p_0 computed in the previous section. We obtain the following set of equations:

$$\begin{aligned} \frac{d\delta p_{\mathbf{k}_L}}{dt} = & -\gamma_{\mathbf{k}_L} \delta p_{\mathbf{k}_L} - 2iE_{int}(\bar{p}_0 \bar{p}_{2\mathbf{k}_L} \delta p_{\mathbf{k}_L}^\dagger + \bar{p}_{\mathbf{k}_L}^* \bar{p}_{2\mathbf{k}_L} \delta p_0 \\ & + \bar{p}_{\mathbf{k}_L}^* \bar{p}_0 \delta p_{2\mathbf{k}_L}) + \delta P_{\mathbf{k}_L}^{in}, \end{aligned} \quad (35)$$

$$\frac{d\delta p_0}{dt} = -\gamma_0 \delta p_0 - iE_{int}(2\bar{p}_{2\mathbf{k}_L}^* \bar{p}_{\mathbf{k}_L} \delta p_{\mathbf{k}_L} + \bar{p}_{\mathbf{k}_L}^2 \delta p_{2\mathbf{k}_L}^\dagger) + \delta P_0^{in}, \quad (36)$$

$$\frac{d\delta p_{2\mathbf{k}_L}}{dt} = -\gamma_{2k_L} \delta p_{2\mathbf{k}_L} - iE_{int}(2\bar{p}_0^* \bar{p}_{\mathbf{k}_L} \delta p_{\mathbf{k}_L} + \bar{p}_{\mathbf{k}_L}^2 \delta p_0^\dagger) + \delta P_{2\mathbf{k}_L}^{in}. \quad (37)$$

We can now inject the mean values of the fields $p_{\mathbf{k}_L}$, p_0 , and $p_{2\mathbf{k}_L}$ that we have computed in the previous section [Eqs. (29), (31), and (32)].

First, we have to choose the phases of the fields (this choice has no influence on the physics of the problem). We set the phase of the pump field $A_{\mathbf{k}_L}^{in}$ to zero. Then $\bar{p}_{\mathbf{k}_L}$ is a positive real number. Equations (26) and (27) impose the same relationship between the signal φ_0 and idler $\varphi_{2\mathbf{k}_L}$ phases,

$$\varphi_0 + \varphi_{2\mathbf{k}_L} = -\frac{\pi}{2}, \quad (38)$$

whereas the relative phase $\varphi_0 - \varphi_{2\mathbf{k}_L}$ is not fixed and undergoes diffusion like the phase of a laser. We set \bar{p}_0 to be a real positive number (this corresponds to neglecting phase diffusion). Then $\bar{p}_{2\mathbf{k}_L}$ is a pure imaginary number. With these choices of phase, the evolution equations write

$$\begin{aligned} \frac{d\delta p_{\mathbf{k}_L}}{dt} = & -\gamma_{k_L} (\delta p_{\mathbf{k}_L} + (\sigma - 1) \delta p_{\mathbf{k}_L}^\dagger) - \sqrt{2\gamma_{k_L} \gamma_0 (\sigma - 1)} \delta p_0 \\ & - i\sqrt{2\gamma_{k_L} \gamma_{2k_L} (\sigma - 1)} \delta p_{2\mathbf{k}_L} + \delta P_{\mathbf{k}_L}^{in}, \end{aligned} \quad (39)$$

$$\begin{aligned} \frac{d\delta p_0}{dt} = & -\gamma_0 \delta p_0 + \sqrt{2\gamma_{k_L} \gamma_0 (\sigma - 1)} \delta p_{\mathbf{k}_L} - i\sqrt{\gamma_0 \gamma_{2k_L}} \delta p_{2\mathbf{k}_L}^\dagger \\ & + \delta P_0^{in}, \end{aligned} \quad (40)$$

$$\begin{aligned} \frac{d\delta p_{2\mathbf{k}_L}}{dt} = & -\gamma_{2k_L} \delta p_{2\mathbf{k}_L} - i\sqrt{2\gamma_{k_L} \gamma_{2k_L} (\sigma - 1)} \delta p_{\mathbf{k}_L} \\ & - i\sqrt{\gamma_0 \gamma_{2k_L}} \delta p_0^\dagger + \delta P_{2\mathbf{k}_L}^{in}. \end{aligned} \quad (41)$$

Using these three equations and their conjugate equations we can calculate the output fluctuations of the pump, signal, and idler fields as a function of the input fluctuations.

B. Amplitude fluctuations

In this paper we are mostly interested in the amplitude correlations between signal and idler.³ We will see that in the simple case where we neglect the renormalization effects it is enough to solve a system of three equations. We define the real and imaginary parts of the polariton, photon, and exciton fields as

$$\begin{aligned}\alpha_{\mathbf{q}} &= \delta p_{\mathbf{q}} + \delta p_{\mathbf{q}}^{\dagger}, \\ \beta_{\mathbf{q}} &= -i(\delta p_{\mathbf{q}} - \delta p_{\mathbf{q}}^{\dagger}), \\ \alpha_{\mathbf{q}}^{in(out)} &= \delta P_{\mathbf{q}}^{in(out)} + \delta P_{\mathbf{q}}^{in(out)\dagger}, \\ \beta_{\mathbf{q}}^{in(out)} &= -i[\delta P_{\mathbf{q}}^{in(out)} - \delta P_{\mathbf{q}}^{in(out)\dagger}], \\ \alpha_{\mathbf{q}}^{A,in(out)} &= \delta A_{\mathbf{q}}^{in(out)} + \delta A_{\mathbf{q}}^{in(out)\dagger}, \\ \beta_{\mathbf{q}}^{A,in(out)} &= -i[\delta A_{\mathbf{q}}^{in(out)} - \delta A_{\mathbf{q}}^{in(out)\dagger}], \\ \alpha_{\mathbf{q}}^{B,in(out)} &= \delta B_{\mathbf{q}}^{in(out)} + \delta B_{\mathbf{q}}^{in(out)\dagger}, \\ \beta_{\mathbf{q}}^{B,in(out)} &= -i[\delta B_{\mathbf{q}}^{in(out)} - \delta B_{\mathbf{q}}^{in(out)\dagger}].\end{aligned}\quad (42)$$

The mean fields $p_{\mathbf{k}_L}$ and p_0 are real positive numbers, therefore $\alpha_{\mathbf{k}_L}$ and α_0 correspond to amplitude fluctuations and $\beta_{\mathbf{k}_L}$ and β_0 to phase fluctuations. The mean field $p_{2\mathbf{k}_L}$ is a pure imaginary number; therefore, $-\beta_{2\mathbf{k}_L}$ corresponds to amplitude fluctuations and $\alpha_{2\mathbf{k}_L}$ to phase fluctuations. The evolution equations for the amplitude fluctuations write

$$\begin{aligned}\frac{d\alpha_{\mathbf{k}_L}}{dt} &= -\gamma_{k_L}\sigma\alpha_{\mathbf{k}_L} - \sqrt{2\gamma_{k_L}\gamma_0(\sigma-1)}\alpha_0 \\ &\quad + \sqrt{2\gamma_{k_L}\gamma_{2k_L}(\sigma-1)}\beta_{2\mathbf{k}_L} + \alpha_{\mathbf{k}_L}^{in},\end{aligned}\quad (43)$$

$$\frac{d\alpha_0}{dt} = -\gamma_0\alpha_0 + \sqrt{2\gamma_{k_L}\gamma_0(\sigma-1)}\alpha_{\mathbf{k}_L} - \sqrt{\gamma_0\gamma_{2k_L}}\beta_{2\mathbf{k}_L} + \alpha_0^{in},\quad (44)$$

$$\begin{aligned}\frac{d\beta_{2\mathbf{k}_L}}{dt} &= -\gamma_{2k_L}\beta_{2\mathbf{k}_L} - \sqrt{2\gamma_{k_L}\gamma_{2k_L}(\sigma-1)}\alpha_{\mathbf{k}_L} - \sqrt{\gamma_0\gamma_{2k_L}}\alpha_0 \\ &\quad + \beta_{2\mathbf{k}_L}^{in}.\end{aligned}\quad (45)$$

We get a set of three linear differential equations. Taking the Fourier transform we obtain in matrix notation

$$\begin{pmatrix} \gamma_{k_L}\sigma - i\Omega & \sqrt{2\gamma_{k_L}\gamma_0(\sigma-1)} & -\sqrt{2\gamma_{k_L}\gamma_{2k_L}(\sigma-1)} \\ -\sqrt{2\gamma_{k_L}\gamma_0(\sigma-1)} & \gamma_0 - i\Omega & \sqrt{\gamma_0\gamma_{2k_L}} \\ \sqrt{2\gamma_{k_L}\gamma_{2k_L}(\sigma-1)} & \sqrt{\gamma_0\gamma_{2k_L}} & \gamma_{2k_L} - i\Omega \end{pmatrix} \times \begin{pmatrix} \alpha_{\mathbf{k}_L}(\Omega) \\ \alpha_0(\Omega) \\ \beta_{2\mathbf{k}_L}(\Omega) \end{pmatrix} = \begin{pmatrix} \alpha_{\mathbf{k}_L}^{in} \\ \alpha_0^{in} \\ \beta_{2\mathbf{k}_L}^{in} \end{pmatrix}.\quad (46)$$

The inversion of the 3×3 matrix provides the amplitude fluctuations of the fields $p_{\mathbf{k}_L}(\Omega)$, $p_0(\Omega)$, and $p_{2\mathbf{k}_L}(\Omega)$ as a function of the input fluctuations.

C. Fluctuations of the output light fields

The intracavity light field for a given wave vector \mathbf{q} can be deduced from the polariton fields by inverting Eq. (5): $a_{\mathbf{q}} = -C_q p_{\mathbf{q}} + X_q q_{\mathbf{q}}$. Thus the spectrum of the intracavity light field fluctuations is given by

$$\delta a_{\mathbf{q}}(\Omega) = -C_q \delta p_{\mathbf{q}}(\Omega) + X_q \delta q_{\mathbf{q}}(\Omega),\quad (47)$$

where $\delta a_{\mathbf{q}}(\Omega)$, $\delta p_{\mathbf{q}}(\Omega)$, and $\delta q_{\mathbf{q}}(\Omega)$ are the Fourier components of the field fluctuations in the rotating frame at the lower polariton frequency $E_p(q)$.

The spectrum of the upper polariton field $q_{\mathbf{q}}$ is peaked around the upper polariton frequency $E_q(q)$. If the upper polariton linewidth is smaller than the splitting $E_q(q) - E_p(q)$ (which we will assume, since it corresponds to the strong-coupling condition), the components of $q_{\mathbf{q}}$ around the lower polariton frequency $E_p(q)$ are very small and can be neglected. Therefore, if we limit ourselves to small enough noise frequencies Ω around the center frequency $E_p(q)$, we have

$$\delta a_{\mathbf{q}}(\Omega) = -C_q \delta p_{\mathbf{q}}(\Omega).\quad (48)$$

It is easy to deduce the fluctuations of the output light field using the input-output relationship for the cavity mirror $A_{\mathbf{q}}^{out} = \sqrt{2\gamma_{aq}}a_{\mathbf{q}} - A_{\mathbf{q}}^{in}$ [15,16]. One finally obtains

$$\delta A_{\mathbf{q}}^{out}(\Omega) = -C_q \sqrt{2\gamma_{aq}} \delta p_{\mathbf{q}}(\Omega) - \delta A_{\mathbf{q}}^{in}(\Omega)\quad (49)$$

or, for the amplitude fluctuations,

$$\alpha_{\mathbf{q}}^{A,out}(\Omega) = -C_q \sqrt{2\gamma_{aq}} \alpha_{\mathbf{q}}(\Omega) - \alpha_{\mathbf{q}}^{A,in}(\Omega).\quad (50)$$

D. Input fluctuations

In this paragraph we study the noise sources in our system. $A_{\mathbf{k}_L}^{in}$ is the coherent pump laser field A_0^{in} and both other input fields $A_{2\mathbf{k}_L}^{in}$ are equal to the vacuum field. Therefore, the amplitude fluctuations of these three fields are equal to the vacuum fluctuations. The treatment of excitonic fluctuation is more complex. The amplitude noise spectra (normalized to the vacuum noise) of the three excitonic fields $B_{\mathbf{k}_L}^{in}$, B_0^{in} , and $B_{2\mathbf{k}_L}^{in}$ are given by

³Correlations between other quadratures of the signal and idler fields are hardly accessible in experiments, because of the large frequency difference between them (a few meV, i.e., a few hundreds of GHz).

$$S_{\alpha_{\mathbf{q}}}^{B,in}(\Omega) = 1 + 2n_{\mathbf{q}} \text{ for } \mathbf{q} = \mathbf{0}, \mathbf{k}_L, 2\mathbf{k}_L, \quad (51)$$

where $n_{\mathbf{q}}$ is the mean number of excitations in the reservoir which depends on the temperature and pump intensity. Since the reservoir is populated through phonon-assisted relaxation from the pump mode it is a reasonable assumption to take the reservoir occupation as proportional to the mean number of excitons in the pump mode

$$n_{\mathbf{q}} = \beta |b_{\mathbf{q}}|^2 = \beta X_q^2 |p_{\mathbf{q}}|^2, \quad (52)$$

where β is a dimensionless constant which characterizes the efficacy of the relaxation process. This simple model accounts for the excess noise of the reflected light at low excitation intensity in a satisfactory way. In particular, it reproduces the observed linear dependence of the excess noise with the excitation intensity [10].

E. Noise spectra

In fluctuation measurements the measured quantity is the noise spectrum. The noise spectrum $S_O(\Omega)$ of an operator O is defined as the Fourier transform of the autocorrelation function $C_O(t, t')$,

$$S_O(\Omega) = \int C_O(\tau) e^{i\Omega\tau} d\tau, \quad (53)$$

where

$$C_O(t, t') = \langle O(t)O(t') \rangle - \langle O(t) \rangle \langle O(t') \rangle = \langle \delta O(t) \delta O(t') \rangle, \quad (54)$$

and for a stationary process $C_O(t, t') = C_O(\tau)$ with $\tau = t - t'$. The noise spectrum is related to the Fourier transform $\delta O(\Omega)$ of the fluctuations $\delta O(t)$ by the Wiener-Kinchine theorem

$$\langle \delta O(\Omega) \delta O(\Omega') \rangle = 2\pi \delta(\Omega + \Omega') S_O(\Omega). \quad (55)$$

In the same way the correlation spectrum $S_{OO'}(\Omega)$ of two operators O, O' is defined as the Fourier transform of the correlation function

$$C_{OO'}(t, t') = \langle O(t)O'(t') \rangle - \langle O(t) \rangle \langle O'(t') \rangle. \quad (56)$$

The correlation spectrum is also related to the Fourier components of the fluctuations

$$\langle \delta O(\Omega) \delta O'(\Omega') \rangle = 2\pi \delta(\Omega + \Omega') S_{OO'}(\Omega). \quad (57)$$

The relevant quantity is the normalized correlation spectrum

$$C_{OO'}(\Omega) = \frac{S_{OO'}(\Omega)}{\sqrt{S_O(\Omega)S_{O'}(\Omega)}}. \quad (58)$$

One has always $|C| \leq 1$. A nonzero value of $C_{OO'}(\Omega)$ indicates some level of correlation between the two measurements.

VI. RESULTS

A. Fluctuations of the intracavity polariton fields

In order to shed some light on the above-mentioned analogy with an OPO, we assume that all three polariton modes

have the same linewidths. This is the case if the cavity and exciton linewidths are equal ($\gamma_{ak} = \gamma_{bk}$) and do not depend on k . We set $\gamma = \gamma_{k_L} = \gamma_0 = \gamma_{2k_L} = \gamma_a = \gamma_b$.

After some straightforward algebra we get the amplitude fluctuations of the polariton fields,

$$\alpha_{\mathbf{k}_L}(\Omega) = \frac{1}{D(\Omega)} [-\gamma(\Omega + 2i\gamma)\alpha_{\mathbf{k}_L}^{in} - \gamma\sqrt{2(\sigma-1)}(2\gamma - i\Omega)\alpha_0^{in} + \gamma\sqrt{2(\sigma-1)}(2\gamma - i\Omega)\beta_{2\mathbf{k}_L}^{in}], \quad (59)$$

$$\alpha_0(\Omega) = \frac{1}{D(\Omega)} \{ \gamma\sqrt{2(\sigma-1)}(2\gamma - i\Omega)\alpha_{\mathbf{k}_L}^{in} + [\gamma^2(3\sigma-2) - \Omega^2 - i\gamma\Omega(\sigma+1)]\alpha_0^{in} + \gamma[\gamma(\sigma-2) + i\Omega]\beta_{2\mathbf{k}_L}^{in} \}, \quad (60)$$

$$\beta_{2\mathbf{k}_L}(\Omega) = \frac{1}{D(\Omega)} \{ -\gamma\sqrt{2(\sigma-1)}(2\gamma - i\Omega)\alpha_{\mathbf{k}_L}^{in} + \gamma[\gamma(\sigma-2) + i\Omega]\alpha_0^{in} + [\gamma^2(3\sigma-2) - \Omega^2 - i\gamma\Omega(\sigma+1)]\beta_{2\mathbf{k}_L}^{in} \}, \quad (61)$$

with

$$D(\Omega) = \gamma[8\gamma^2(\sigma-1) - \Omega^2(\sigma+2)] + i\Omega[\gamma^2(4-6\sigma) + \Omega^2]. \quad (62)$$

B. Twin polaritons

Let us now calculate the fluctuations of the difference of the signal and idler amplitudes. Let r be the normalized quantity

$$r(\Omega) = \frac{1}{\sqrt{2}} [\alpha_0(\Omega) + \beta_{2\mathbf{k}_L}(\Omega)]. \quad (63)$$

The plus sign comes from the fact that the idler amplitude fluctuation is $-\beta_{2\mathbf{k}_L}$. We find

$$r(\Omega) = [4\gamma^2(\sigma-1) - \Omega^2 - i\Omega\gamma\sigma] r^{in} \quad (64)$$

with

$$r^{in} = \frac{1}{\sqrt{2}} (\alpha_0^{in} + \beta_{2\mathbf{k}_L}^{in}).$$

It is important to notice that r does not depend on the pump fluctuations, which cancel out when we make the difference. This property is at the origin of twin beams generation in OPOs. We get perfect noise suppression for $\Omega=0$ and $\sigma \rightarrow 1$.

In a degenerate or quasidegenerate OPO the symmetry between signal and idler is conserved outside the cavity, because the two fields have the same frequency and are coupled in the same way to the external field through the losses of the cavity mirrors. In such systems the twin character of the signal and idler fields can be shown directly by measuring the fluctuations of the difference of the output signal and idler field intensities.

In our case the signal and idler polaritons do not have the same photon fraction and are not coupled in the same way to

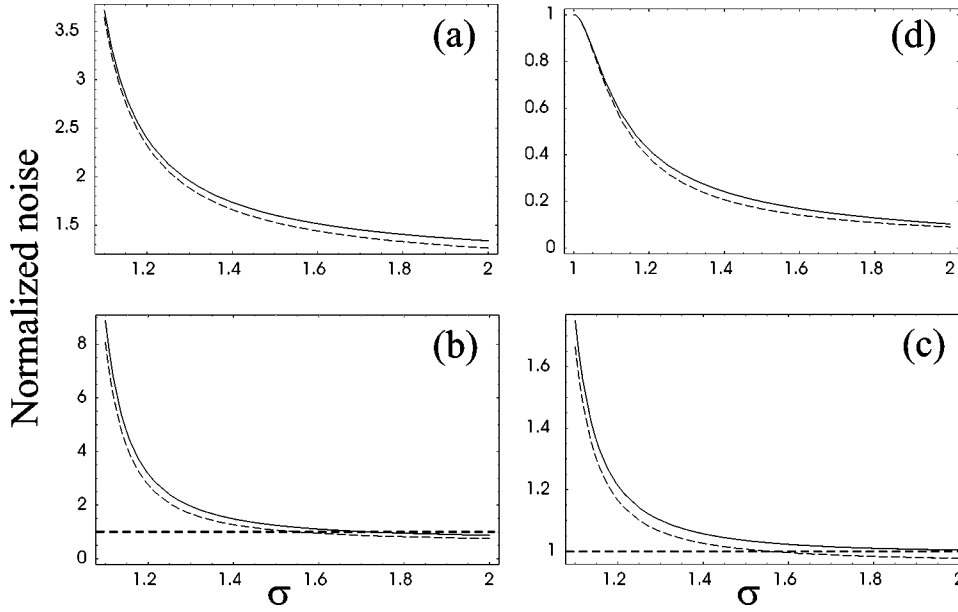


FIG. 5. (a)–(c) Amplitude noises at zero frequency of the pump, signal, and idler beams, respectively. (d) Signal-idler amplitude correlation at zero frequency as a function of the pump parameter σ . The three modes are assumed to have the same linewidths. The input excess noises for each mode are given by the value of the β coefficient [see Eq. (52)]. Dashed line: ideal case $\beta = 0$ (the input noises are set as equal to the standard quantum noise). Solid line: $\beta = 5 \times 10^{-5}$.

the external field. Clearly, this should lead to a significant reduction of the correlations between the signal and idler output light fields.

C. Fluctuations of the output light fields

Let us first comment on the relevant frequency for the noise analysis. The noise spectra vary typically over a range of the order of the polariton linewidth. In noise measurements, experimentalists have access to very small analyses frequencies (generally a few tens of MHz, i.e., a fraction of μeV) with respect to the polariton linewidths (a few hundreds of μeV). Therefore the noise at zero frequency is the relevant quantity. In the following we will concentrate on the study of the noise at zero frequency.

The general expressions of the noise spectra of the three modes and of the signal-idler amplitude correlation can be found in the Appendix. In the preceding section we have taken equal linewidths for the pump, signal, and idler polaritons ($\gamma_{k_L} = \gamma_0 = \gamma_{2k_L}$). This assumption is not correct in most microcavity samples. Indeed the energy of the polaritons of wave vector $2\mathbf{k}_L$ is close to the energy of the nonradiative excitons; scattering towards these states is enhanced by their large density of states. Moreover, the idler energy is closer to the electron-hole continuum. As a result, the *excitonic* linewidth of the idler γ_{b2k_L} is larger than that of the signal γ_{b0} and pump γ_{bk_L} modes. The assumption that the *cavity* linewidth γ_{ak} does not depend on k is correct, provided that the three wave vectors of interest are within the stop band of the Bragg reflectors. In recent experiments, the idler beam has been found to be about 50 times weaker than the signal beam (see, e.g., Ref. [5]), which is consistent with a linewidth ratio of $\gamma_{2k_L}/\gamma_0 = 5$.

We will give the results in the ideal case (with equal linewidths and an input noise equal to the standard quantum noise), and then study the influence of the imbalance between signal and idler, and the input excitonic noise.

1. Ideal case

In the case of equal linewidths (and no input excess noise) the general expressions given in the Appendix reduce to a simpler form,

$$S_{\alpha_{k_L}}^{A,out} = 1 + C_{k_L}^2 \frac{1}{\sigma - 1}, \quad (65)$$

$$S_{\alpha_0}^{A,out} = 1 + C_0^2 \frac{7\sigma^2 + 16\sigma - 8}{8(\sigma - 1)^2}, \quad (66)$$

$$S_{\beta_{2k_L}}^{A,out} = 1 + C_{2k_L}^2 \frac{-7\sigma^2 + 16\sigma - 8}{8(\sigma - 1)^2}, \quad (67)$$

$$S_{\alpha_0 - \beta_{2k_L}}^{A,out} = C_0 C_{2k_L} \frac{\sigma^2}{8(\sigma - 1)^2}. \quad (68)$$

The amplitude noises of the pump, signal, and idler beams, as well as the signal-idler normalized amplitude correlation, are drawn in Fig. 5 as a function of the pump parameter $\sigma = \sqrt{I_{k_L}^{in}/I_{k_L,thr}^{in}}$. Although the curves go up to $\sigma = 2$, let us recall that the model is not correct too far above threshold, where we can no longer neglect multiple diffusions.

Let us observe that the signal and idler noise spectra have exactly the same shape. However, the idler noise is closer to the standard quantum level than the signal noise is, due to its low photon fraction which causes important losses at the output of the cavity. The ratio of the excess noises $S - 1$ is simply equal to the ratio of the photon fractions

$$\frac{S_{\alpha_0}^{A,out}(\Omega) - 1}{S_{\beta_{2k_L}}^{A,out}(\Omega) - 1} = \frac{C_0^2}{C_{2k_L}^2}. \quad (69)$$

The signal and idler amplitude fluctuations diverge close to the threshold (for $\sigma \rightarrow 1^+$). Noise reduction is obtained above $\sigma = 1.55$. It grows with the pump intensity and satu-

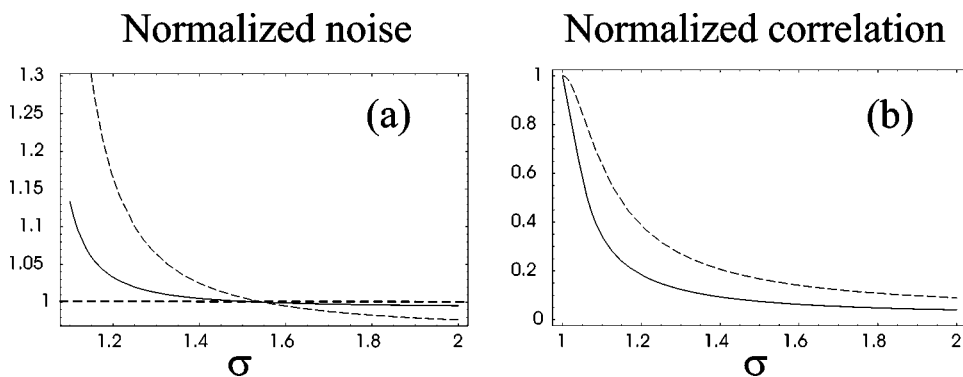


FIG. 6. (a) Amplitude noise of the idler beam and (b) signal-idler correlation at zero frequency as a function of pump intensity for $\gamma_{2k_L} = 5\gamma_0$. On both plots, the curve in the dashed line is the “balanced” case $\gamma_{2k_L} = \gamma_0$.

rates at a maximum value of $7C_0^2/8$ for the signal beam ($7C_{2k_L}^2/8$ for the idler beam). The signal and idler amplitudes are very strongly correlated slightly above threshold. The correlation tends to one in the vicinity of the threshold ($\sigma \rightarrow 1^+$) and vanishes rapidly when increasing the pump intensity. All these results are similar to those obtained in nondegenerate OPOs [28].

2. Influence of the signal-idler imbalance

In this paragraph we still suppose that there is no input excess noise ($n_0 = n_{k_L} = n_{2k_L} = 0$). Let us compare the results with different linewidths to those of the “balanced” case ($\gamma = \gamma_k = \gamma_0 = \gamma_{2k_L} = \gamma_a = \gamma_b$) in Eqs. (A1)–(A4). It is easy to show that the excess noises $S-1$ of the pump, signal, and idler beams are respectively multiplied by γ_a/γ_{k_L} , γ_a/γ_0 , and γ_a/γ_{2k_L} . The signal-idler correlation (without normalization) is multiplied by $\gamma_a/\sqrt{\gamma_0\gamma_{2k_L}}$.

As an example the case $\gamma_0 = \gamma_{k_L} = \gamma_{2k_L}/5 = \gamma_a$ is shown in Fig. 6. The amplitude noises of the pump and signal beams have not been represented since they are unchanged. The excess noise and noise reduction are strongly reduced on the idler beam due to its larger losses [Fig. 6(a)]. The signal-idler correlation remains strong close to threshold but decreases more rapidly with increasing pump intensity [Fig. 6(b)].

3. Influence of input excess noise

We have assumed that the largest source of noise for a given polariton mode is the luminescence of an exciton reservoir, which is populated by the polariton mode itself. The input noise for a given mode is then proportional to the mean exciton number in this mode. The efficiency of this process is given by the β coefficient introduced above [see Eq. (52)]. Here we will assume that β has the same value for the three modes. Slightly above the oscillation threshold, the pump mode is much more populated than the signal and idler population; then the input noise is much greater for the pump than for the signal and idler.

Figure 5 shows an example in the “balanced” case for a noise parameter $\beta = 5 \times 10^{-5}$, evaluated from noise measurements on the light reflected by a microcavity sample [10]. The input excess noise cuts down the noise reduction. Its influence increases with the pump intensity since it is proportional to the mean exciton population. However, the correlation is actually enhanced by the excess noise. It is due to

the fact that the pump input noise is distributed equally between signal and idler, and contributes to the correlations.

D. The quantum domain

Our model predicts strong correlations between the signal and idler light fields. When can we say that these beams are quantum correlated? We will use two different criteria, one evaluating the “quantum twin” character of the beams and one associated with QND measurements.

1. Twin character

In degenerate or quasidegenerate OPOs, the signal and idler output beams have the same mean-field values and the same noise properties. Quantum correlations between them are evidenced by measuring the noise of the difference between signal and idler intensities and comparing it to the standard quantum level. The idea behind this is to compare the fields under consideration to a classical production of twin beams, which can be achieved by using a 50% beam splitter.

In our case, one beam is much more intense than the other one (the ratio of the intensities is of the order of 10 for equal signal and idler linewidths). What happens if the two light fields A_1 and A_2 under consideration have different mean values and different noises S_1 and S_2 ? To produce classically twin beams of unequal intensities, one can use an unequal beam splitter. The field fluctuations at the output of such a beam splitter can be written as

$$\delta A_1 = t\delta A_{in} + r\delta A_v, \quad (70)$$

$$\delta A_2 = r\delta A_{in} - t\delta A_v, \quad (71)$$

with $t \neq r$, where A_{in} is the input field and δA_v the vacuum fluctuations entering through the other port of the beam splitter. Now the difference $\delta A_- = \delta A_1 - \delta A_2$ is not relevant for our purpose, since it does not give a quantity which is independent of δA_{in} , the noise of the beam which has been used to produce the twin fields. However, one has in this case the following relation which is independent of δA_{in} :

$$\langle \delta A_1 \delta A_2 \rangle_{class}^2 = (\langle \delta A_1^2 \rangle - 1)(\langle \delta A_2^2 \rangle - 1). \quad (72)$$

Then the normalized correlation can be written as

$$(C_{class})^2 = \left(1 - \frac{1}{S_1}\right) \left(1 - \frac{1}{S_2}\right). \quad (73)$$

It is equal to zero if the noise of the input beam is the vacuum noise and increases towards 1 with the excess noise of the input beam. We would now like to evaluate the twin character of the beams by using a quantity which would be smaller than 1 if the two beams are more strongly correlated than the copies from a beam splitter, just like the usual squeezing factor on the intensity difference. From Eq. (73) it can be seen that the quantity

$$G = \frac{1 - C}{1 - \sqrt{\left(1 - \frac{1}{S_1}\right) \left(1 - \frac{1}{S_2}\right)}} \quad (74)$$

satisfies this condition. Moreover, it is possible to show that the “quantum twin” criterion $G < 1$ does not depend on the way by which the two classical twins are produced [30]. Thus G is indeed a useful generalization of the squeezing factor on the intensity difference that allows us to treat the case of beams of unequal intensities.

Experimentally, one can measure separately C , S_1 , and S_2 and compute G from (74). One can also amplify in a different way the two photocurrents (with gains a and $1/a$, respectively) before measuring the noise on the intensity difference; the measured fluctuation is then $\delta A_a = a \delta A_1 - \delta A_2/a$. If we choose $a^2 = \sqrt{S_2/S_1}$, we find that G is proportional to the photocurrent fluctuations

$$G = \frac{\langle \delta A_a^2 \rangle}{2} \frac{1}{\sqrt{S_1 S_2} - \sqrt{(S_1 - 1)(S_2 - 1)}}. \quad (75)$$

Thus, one has direct access to G provided the gains are adjusted so that the noise levels are identical in the two channels. The denominator in (75) can be evaluated from the excess noises of each field.

2. QND correlation

A further level of correlation is achieved when the information extracted from the measurement of one field provides a QND measurement of the other, so that it is possible, using the information on one field, to correct the other from a part of its quantum fluctuations and transform it into a squeezed state. This criterion is widely used in the field of QND measurement [29]. It can be expressed in terms of the conditional variance

$$V_{1|2} = S_1(1 - C^2). \quad (76)$$

Note that when the two beams have different noises ($S_1 \neq S_2$) one has two conditional variances and, therefore, two possible criteria. This shows that the QND criterion evaluates the correlation from the point of view of one beam, and is not an evaluation of the quantum correlation between the two fields. One possibility is to state that the two fields are QND-correlated if one has $V_{1|2} < 1$ and $V_{2|1} < 1$. This criterion is stronger than the previous one [30]. In the following, we will discuss these two quantum criteria in the case of the

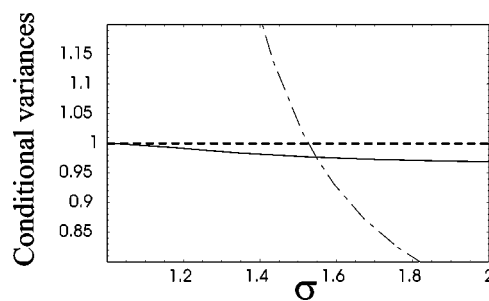


FIG. 7. Dash-dotted line: the conditional variance of the signal intensity fluctuations, knowing those of the idler. Solid line: the conditional variance of the idler intensity fluctuations, knowing those of the signal. The dashed line is the standard quantum level.

signal and idler beams produced by a semiconductor microcavity.

3. Discussion

We investigate the “QND criterion.” The conditional variances are shown in Fig. 7 in the case of equal linewidths and zero input excess noise. From the point of view of the idler beam, the conditional variance is always lower than 1, if only by a few percent. From the point of view of the signal beam, the quantum domain is very small: it begins at $\sigma = 1.53$, very close to the point where it begins to be squeezed. It is only between $\sigma = 1.53$ and $\sigma = 1.55$ that we get “QND correlations” between beams that individually have excess noise. For $\sigma > 1.55$, the QND-correlation criterion is satisfied, although the correlation is quite small, because both beams are squeezed. In conclusion, no significant “QND correlations” can be observed on the signal and idler output beams.

We now investigate the behavior of the quantity G by evaluating the twin character of the signal and idler beams. It is drawn in Fig. 8 as a function of the pump parameter in various cases. In the case of equal linewidths and zero input excess noise, G goes down to 0.85, which indicates the “quantum twin” character of the two beams. If we take the nonradiative losses of the idler polaritons into account (we set again $\gamma_{2k_L} = 5\gamma_0$), G only goes under 1 by 7%. However,

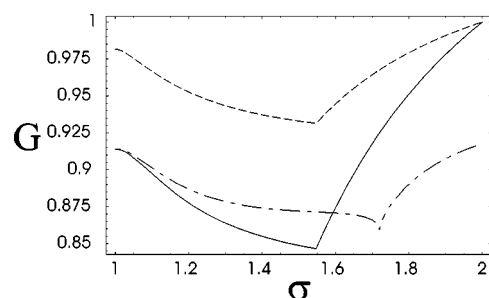


FIG. 8. Value of the quantity G as a function of the pump parameter, in three different cases. (a) Solid line: ideal case where all linewidths are equal and there is no excess noise. (b) Dashed line: different linewidths for the signal and idler modes $\gamma_{2k_L} = 5\gamma_0$, and no excess noise. (c) Dash-dotted line: all linewidths are equal, and some excess noise is given by $\beta = \beta_c/2$.

the input excess noise (corresponding to the resonant luminescence of the three polariton modes) has little effect on the quantum correlations. As explained above, this comes from the fact that the pump input noise (which is the strongest slightly above threshold, when the pump polariton population is much larger than the signal and idler populations) is equally distributed between the signal and idler modes and helps build up classical (but not quantum) correlations.

In conclusion, in present-day microcavity samples the “quantum twin” criterion is overcome by only a few percent. This is due to the fact that only the polariton fields are perfectly correlated, and we can only observe their photonic parts. A simple image is the following: we observe the polariton system through a beamsplitter which amplitude transmission coefficient is equal to the Hopfield coefficient C_0 , which leads to losses that destroy the quantum effects. The correlations are further reduced by the imbalance between signal and idler. The photonic part of the idler is very small (of the order of 0.05), which corresponds to large losses.

VII. CONCLUSION

We have presented a quantum model allowing us to calculate the quantum fluctuations of the beams produced by a semiconductor microcavity in the regime of parametric oscillation. It extends the model developed by Ciuti *et al.* above threshold and includes the noise coming from the exciton part of the polaritons.

We show that some quantum correlation exists between the signal and idler beams in the vicinity of threshold. Taking the parameters of microcavity samples, which have been shown to work in the parametric oscillation regime, it can be seen that the correlation overcomes the quantum limit by a few percent. The measurement of these correlations would be of great interest, since quantum correlations between the output beams, however small, are an indication of much bigger correlations between the intracavity polariton fields. For example, in the ideal case at threshold (see Fig. 8), if we measure $G=0.91$, this corresponds to perfect correlations inside the cavity.

In order to observe better quantum correlations between the output beams, it is very important that the signal and idler linewidths be made as equal as possible. A simple solution would be to use a low-finesse cavity. Then the nonradiative losses would be less important with respect to the radiative losses, and the ratio of the signal and idler linewidths would be smaller. A compromise has to be found because the oscillation threshold would also be higher.

We acknowledge fruitful discussions with C. Fabre, C. Ciuti, P. Schwendimann, and A. Quattropani.

APPENDIX: NOISE AND SIGNAL-IDLER CORRELATION

In this section, we give the general expressions for the amplitude noises of the signal, pump, and idler output light

fields at zero frequency (denoted by $S_{\alpha_0}^{A,out}$, $S_{\alpha_{\mathbf{k}_L}}^{A,out}$, and $S_{\beta_{2\mathbf{k}_L}}^{A,out}$, respectively), and the signal-idler amplitude correlation at zero frequency (denoted by $S_{\alpha_0 \beta_{2\mathbf{k}_L}}^{A,out}$).

First, the polariton field amplitude fluctuations are calculated by inverting Eq. (46). Then, the amplitude fluctuations of the output fields are given by Eq. (50). Finally, the amplitude noise and correlation spectra are calculated using Eqs. (55) and (57), respectively.

$$S_{\alpha_{\mathbf{k}_L}}^{A,out} = 1 + C_{k_L}^2 \frac{\gamma_a}{\gamma_{k_L}} \frac{1}{\sigma - 1} \times \left(1 + \frac{X_0^2 n_0 \gamma_{b0} \gamma_{2k_L} + X_{2k_L}^2 n_{2\mathbf{k}_L} \gamma_{b2k_L} \gamma_0}{\gamma_0 \gamma_{2k_L}} \right), \quad (\text{A1})$$

$$S_{\alpha_0}^{A,out} = 1 + C_0^2 \frac{\gamma_a}{\gamma_0} \frac{1}{8(\sigma - 1)^2} \left\{ -7\sigma^2 + 16\sigma - 8 + \frac{1}{\gamma_{k_L} \gamma_0 \gamma_{2k_L}} \times [8(\sigma - 1) X_{k_L}^2 n_{\mathbf{k}_L} \gamma_{bk_L} \gamma_0 \gamma_{2k_L} + (3\sigma - 2)^2 \times X_0^2 n_0 \gamma_{b0} \gamma_{k_L} \gamma_{2k_L} + (\sigma - 2)^2 X_{2k_L}^2 n_{2\mathbf{k}_L} \gamma_{b2k_L} \gamma_{k_L} \gamma_0] \right\}, \quad (\text{A2})$$

$$S_{\beta_{2\mathbf{k}_L}}^{A,out} = 1 + C_{2k_L}^2 \frac{\gamma_a}{\gamma_{2k_L}} \frac{1}{8(\sigma - 1)^2} \left\{ -7\sigma^2 + 16\sigma - 8 + \frac{1}{\gamma_{k_L} \gamma_0 \gamma_{2k_L}} [8(\sigma - 1) X_{k_L}^2 n_{\mathbf{k}_L} \gamma_{bk_L} \gamma_0 \gamma_{2k_L} + (\sigma - 2)^2 X_0^2 n_0 \gamma_{b0} \gamma_{k_L} \gamma_{2k_L} + (3\sigma - 2)^2 \times X_{2k_L}^2 n_{2\mathbf{k}_L} \gamma_{b2k_L} \gamma_{k_L} \gamma_0] \right\}, \quad (\text{A3})$$

$$S_{\alpha_0 \beta_{2\mathbf{k}_L}}^{A,out} = C_0 C_{2k_L} \frac{\gamma_a}{\sqrt{\gamma_0 \gamma_{2k_L}}} \frac{1}{8(\sigma - 1)^2} \times \left\{ \sigma^2 - \frac{1}{\gamma_{k_L} \gamma_0 \gamma_{2k_L}} [(\sigma - 2)(3\sigma - 2) \times (X_0^2 n_0 \gamma_{b0} \gamma_{k_L} \gamma_{2k_L} + X_{2k_L}^2 n_{2\mathbf{k}_L} \gamma_{b2k_L} \gamma_{k_L} \gamma_0) - 8(\sigma - 1) X_{k_L}^2 n_{\mathbf{k}_L} \gamma_{bk_L} \gamma_0 \gamma_{2k_L}] \right\}, \quad (\text{A4})$$

where n_0 , $n_{\mathbf{k}_L}$, and $n_{2\mathbf{k}_L}$ are the input excitonic noises. From these expressions, it is easy to calculate the normalized signal-idler correlation at zero frequency $C_{\alpha_0 \beta_{2\mathbf{k}_L}}^{A,out}(\Omega)$ using definition (58).

- [1] C. Weisbuch, M. Nishioka, A. Ishikawa, and Y. Arakawa, *Phys. Rev. Lett.* **69**, 3314 (1992).
- [2] R. Houdré, C. Weisbuch, R. P. Stanley, U. Oesterle, P. Pellandini, and M. Ilegems, *Phys. Rev. Lett.* **73**, 2043 (1994).
- [3] P. G. Savvidis, J. J. Baumberg, R. M. Stevenson, M. S. Skolnick, D. M. Whittaker, and J. S. Roberts, *Phys. Rev. Lett.* **84**, 1547 (2000).
- [4] R. M. Stevenson, V. N. Astratov, M. S. Skolnick, D. M. Whittaker, M. Emam-Ismaïl, A. I. Tartakovskii, P. G. Savvidis, J. J. Baumberg, and J. S. Roberts, *Phys. Rev. Lett.* **85**, 3680 (2000).
- [5] J. J. Baumberg, P. G. Savvidis, R. M. Stevenson, A. I. Tartakovskii, M. S. Skolnick, D. M. Whittaker, and J. S. Roberts, *Phys. Rev. B* **62**, R16247 (2000).
- [6] G. Messin, J. Ph. Karr, H. Eleuch, J. M. Courty, and E. Giacobino, *J. Phys.: Condens. Matter* **11**, 6069 (1999); H. Eleuch, J. M. Courty, G. Messin, C. Fabre, and E. Giacobino, *J. Opt. B: Quantum Semiclassical Opt.* **1**, 1 (1999).
- [7] J. Ph. Karr, A. Baas, R. Houdré, and E. Giacobino, *Phys. Rev. A* **69**, 031802 (2004).
- [8] S. Savasta, R. Girlanda, and G. Martino, *Phys. Status Solidi A* **164**, 85 (1997).
- [9] P. Schwendimann, C. Ciuti, and A. Quattropani, *Phys. Rev. B* **68**, 165324 (2003).
- [10] J. Ph. Karr, Ph.D. thesis, Paris, 2001, <http://tel.ccsd.cnrs.fr/>
- [11] J. Mertz, T. Debuisschert, A. Heidmann, C. Fabre, and E. Giacobino, *Opt. Lett.* **16**, 1234 (1991).
- [12] D. M. Whittaker, *Phys. Rev. B* **63**, 193305 (2001).
- [13] C. Ciuti, P. Schwendimann, B. Deveaud, and A. Quattropani, *Phys. Rev. B* **62**, R4825 (2000).
- [14] C. Ciuti, P. Schwendimann, and A. Quattropani, *Phys. Rev. B* **63**, 041303(R) (2001).
- [15] M. J. Collett and C. W. Gardiner, *Phys. Rev. A* **30**, 1386 (1984).
- [16] S. Reynaud and A. Heidmann, *Opt. Commun.* **71**, 209 (1989).
- [17] A. Baas, J. Ph. Karr, H. Eleuch, and E. Giacobino, *Phys. Rev. A* **69**, 023809 (2004).
- [18] D. F. Walls and G. J. Milburn, *Quantum Optics* (Springer-Verlag, Berlin, 1994).
- [19] R. Houdré, C. Weisbuch, R. P. Stanley, U. Oesterle, and M. Ilegems, *Phys. Rev. Lett.* **85**, 2793 (2000).
- [20] C. Ciuti, V. Savona, C. Piermarocchi, A. Quattropani, and P. Schwendimann, *Phys. Rev. B* **58**, 7926 (1998).
- [21] C. Piermarocchi, F. Tassone, V. Savona, A. Quattropani, and P. Schwendimann, *Phys. Rev. B* **53**, 15834 (1996).
- [22] F. Tassone, C. Piermarocchi, V. Savona, A. Quattropani, and P. Schwendimann, *Phys. Rev. B* **56**, 7554 (1997).
- [23] F. Tassone and Y. Yamamoto, *Phys. Rev. B* **59**, 10830 (1999).
- [24] P. G. Savvidis, C. Ciuti, J. J. Baumberg, D. M. Whittaker, M. S. Skolnick, and J. S. Roberts, *Phys. Rev. B* **64**, 075311 (2001).
- [25] A. I. Tartakovskii, D. N. Krizhanovskii, D. A. Kurysh, V. D. Kulakovskii, M. S. Skolnick, and J. S. Roberts, *Phys. Rev. B* **65**, 081308(R) (2002).
- [26] C. Fabre, E. Giacobino, A. Heidmann, and S. Reynaud, *J. Phys. (France)* **50**, 1209 (1989).
- [27] D. Grandclément, G. Grynberg, and M. Pinard, *Phys. Rev. Lett.* **59**, 44 (1989).
- [28] S. Reynaud, A. Heidmann, E. Giacobino, and C. Fabre, in *Progress in Optics*, edited by E. Wolf (Elsevier Science, New York, 1992), Vol. XXX.
- [29] J. Ph. Poizat, J. F. Roch, and Ph. Grangier, *Ann. Phys. (Paris)* **19**, 265 (1994).
- [30] C. Fabre (private communication).